Groundwater for Sustainable Development 29 (2025) 101424

Contents lists available at ScienceDirect

Groundwater for Sustainable Development

journal homepage: www.elsevier.com/locate/gsd

Research paper

# Would mixed physical barriers be able to desalinate coastal aquifers from seawater intrusion under pumping conditions?

Ismail Abd-Elaty [a], Ashraf Ahmed [b,*]

[a] Department of Water and Water Structures Engineering, Faculty of Engineering, Zagazig University, Zagazig, 44519, Egypt
[b] Department of Civil and Environmental Engineering, Brunel University London, Kingston Lane, Uxbridge, UB83PH, United Kingdom

## HIGHLIGHTS

- Layered coastal aquifers have high desalination rates compared to homogenous cases.
- Aquifers with low-k at the bottom showed smaller SWI compared with cases low-k at the top and the middle.
- Desalination reached +27% after installing the mixed physical barrier.
- Groundwater salinity changed by +25%,-0.30% and −60% with pumping 10, 15 and 20 m$^3$/day.

## GRAPHICAL ABSTRACT

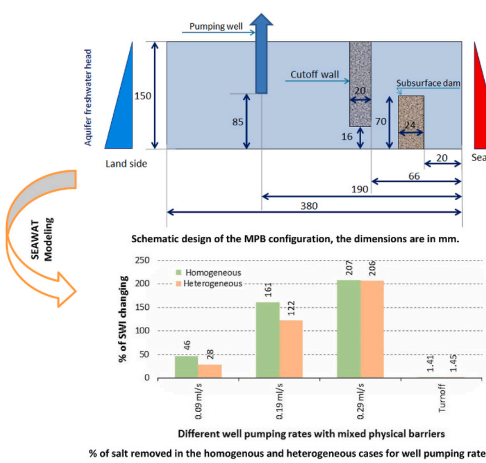


## ARTICLE INFO

*Keywords:*
Aquifer desalination
Mixed physical barriers
Abstraction wells
Field studies
SLR
SEAWAT

## ABSTRACT

This study used the SEAWAT model to investigate the potential of using mixed physical barriers (MPB) to control SWI under pumping conditions in typical homogenous and layered heterogeneous coastal aquifers. The numerical models were based on controlled two-dimensional (2D) laboratory tests and field studies in the Biscayne aquifer, which is situated in the Cutler Ridge region close to Deering Estate, Florida, USA. The modelling results revealed critical insights into SWI behaviour under pumping conditions. Specifically, it was observed that the intrusion wedge extended significantly further inland in layered heterogeneous aquifers and homogeneous aquifers compared with the base case without pumping. Results showed that coastal aquifers with bottom low-hydraulic conductivity have smaller SWI compared with top and middle-layered aquifers. The SWI repulsion reached 27% by installing the MPB, while the groundwater salinity increased to 3%, 38% and 121% by increasing the abstraction well rates by 10 m$^3$/day, 15 m$^3$/day and 20 m$^3$/day, compared with no pumping after using the MPB. The current study results are very interesting for coastal aquifer management and require economic study to ensure the feasibility of using this method.

* Corresponding author.
*E-mail addresses:* Eng_abdelaty2006@yahoo.com (I. Abd-Elaty), ashraf.ahmed@brunel.ac.uk (A. Ahmed).

https://doi.org/10.1016/j.gsd.2025.101424
Received 3 October 2024; Received in revised form 27 January 2025; Accepted 16 February 2025
Available online 21 February 2025

**Notations**

| | |
|---|---|
| IMT | Integrated MT3DMS Transport |
| HFE | Hydrochemical Facies Evolution |
| MODFLOW | United States Geological Survey modular finite-difference flow model |
| MT3DMS | Modular Transport Three-Dimensional Multi-Species |
| MSL: | Mean Sea Level |
| MPSB | mix physical barriers |
| PSB | Physical Surface Barriers |
| SWI | Saltwater Intrusion |
| SUTRA | A three-dimensional, variable-density solute-transport model |
| SWAT | Soil and Water Assessment Tool |
| SEAWAT | Three-Dimensional Variable-Density Groundwater Flow |
| 2D | 2 Dimensions |
| 3D | 3 Dimensions |
| USA: | United States of America |
| VDF | Variable-Density Flow |

## 1. Introduction

Saltwater intrusion (SWI) management becomes necessary to protect coastal groundwater resources from salinisation (Abd-Elaty et al., 2024). Around 95% of the world's coastal areas will be severely affected by sea level rise by 2100, increasing the risk of flooding and SWI (Agren and Svensson, 2007). Climate change and overpopulation are increasing the water demand annually and growing, which draws worldwide attention to the freshwater saline water crisis (Abd-Elaty et al., 2021). Many researchers studied saltwater intrusion in coastal aquifers. Badan Ghyben (1889) attempted the first SWI model, known as the Ghyben- Herzberg model. This model assumes that fresh and saltwater are immiscible and separated by a sharp interface. Henry (1964) developed the first analytical solution for steady-state conditions, including the effect of dispersion in a confined aquifer. El Fleet and Baird (2001) developed a 2-D sharp interface model to investigate the impact of overabstraction on SWI. The model was also applied to a coastal aquifer in Tripoli, Libya.

Ojeda et al. (2004) used the SUTRA code to simulate the saline-fresh water interface in the Yucatan peninsula aquifer. They found the interface position was very sensitive to the pumping well depth and distance from the coastline. The SWI problem was successfully studied by Frind (1982), Cheng et al. (1998), Taylor et al. (2001) and Fahs et al. (2018). The numerical models were applied to the problem, including (Abdoulhalik et al., 2017, 2024), who first introduced and applied the MPB, which consists of a semi-permeable subsurface dam and an impermeable cutoff wall. The results showed that the MPB effectively controls SWI more than the traditional single barrier, such as cutoff walls or subsurface dams. Pisinaras et al. (2021) simulated groundwater salinisation due to SWI using a combination of the Soil and Water Assessment Tool (SWAT) and SEAWAT model. They found that high variability in groundwater recharge diminished the quality and quantity of aquifer water supply. Panthi et al. (2022) showed that coastal aquifers are an active research area in the contiguous United States. The results showed that the drivers of SWI are increasingly better understood and quantified, and the need for increased monitoring is also recognised. Also, the number of monitoring sites has not increased significantly over the review period. Goswami and Rai (2024) indicated that the seawater mixing index reveals that ~34.5% of samples are of relatively freshwater types, while ~61% of samples appear contaminated to some extent, presumably due to the mixing of seawater, or anthropogenic activities such as mining and agricultural activities, Also, analysis of the Hydrochemical Facies Evolution diagram showed that ~23% of samples are directly affected by SWI. Mueller et al. (2024) showed the adverse impact of using saline drinking water and that people are at greater risk of high blood pressure and potentially other adverse health outcomes. The study showed that the first is any coastal areas with projected inland saltwater intrusion of ≥1 km inland, the second is more than 50% of the population in coastal secondary administrative areas with reliance on groundwater for drinking water, and the third is high national average sodium urinary excretion (i.e., > 3 g/day). Moreover, the study identified 41 nations across all continents (except Antarctica) that will be within ≥1 km of inland saltwater intrusion by 2050.

Mitigation of SWI in coastal aquifers has been carried out through different methods to make a balance between the fresh groundwater and saline water hydrostatic heads. The first method is the hydraulic method, which reduces pumping rates, relocates pumping well systems, and increases groundwater recharge by both natural and artificial techniques. Hydraulic methods also include the abstraction of saline water and recharging of desalinated water or treated wastewater recharge (e.g. Pool and Carrera, 2010). The second method is physical barriers, including cutoff walls, subsurface dams and mixed physical barriers (e.g. Abdoulhalik et al., 2017, 2024). Combining the physical subsurface barriers and well recharge to minimise the evaporation from a storage dam and an artificial lake in semi-arid and semi-humid could reduce the SWI considerably (Manga et al., 2012; Mays, 2010; Zheng et al., 2021).

Gao et al. (2022) recently investigated the influence of using cutoff walls dynamic mechanisms of nitrate accumulation and denitrification in a stratified heterogeneous aquifer. The results showed that the stratification pattern greatly disrupted groundwater flow and significantly increased nitrate accumulation. Abd-Elaty et al. (2022) simulated the management of coastal aquifer salinity using inclined physical subsurface barriers. The results showed that the most positive impact was achieved for a wall slope of 1/4, indicating that a moderate vertical inclination of the physical subsurface barriers better preserved coastal groundwater resources. Wang et al. (2023) showed that the installation of a mixed physical barrier (MPB) resulted in an exacerbation of nitrate concentration and the area of nitrate contamination within the aquifer. However, they demonstrated that, regarding SWI control, the MPB was 46–53% and 16–57% more effective than traditional subsurface dams and cutoff walls, respectively. The construction of the MPB resulted in more severe nitrate pollution accumulation. Specifically, the MPB induced 14–27% and 2–12% more nitrate accumulation than conventional subsurface dams and cutoff walls. Their findings highlight the importance of careful design selection in constructing MPB to limit the accumulation of nitrate pollutants without compromising its performance in controlling SWI. Emara et al. (2024) applied the SEAWAT code to assess the impact of aquifer stratification on MPB effectiveness and their response to structural variations in coastal aquifers. The results showed that MPBs efficiently decrease SWI wedge length by up to 65% in all cases. Abdoulhalik et al. (2022) studied the protective effect of cutoff walls on groundwater pumping against saltwater upconing in coastal aquifers. The results highlighted that the penetration depth of the cutoff walls may not necessarily need to exceed the depth of the pumping well to ensure effectiveness, which is of great importance from construction and economic perspectives. Abdoulhalik et al. (2024) studied the effects of layered heterogeneity on mixed physical barrier performance to prevent seawater intrusion in coastal aquifers. The results showed comparable performance when the high K layer was confined between two low K layers or when the aquifer presented a monotonically increasing/decreasing K pattern.

The investigation of saltwater intrusion in coastal aquifers under the pumping conditions in homogenous and layered heterogeneous aquifers using MPB needs to be evaluated. The current study aims to apply MPB to mitigate SWI using numerical simulations by using SEAWAT. The numerical study was carried out based on the laboratory experiments conducted on a 2D-laboratory scale and developed by Abdoulhalik et al. (2017). The ability of MPB was examined for heterogeneous layered aquifers, with the top and bottom layers having high permeability and the middle layer having low permeability interlayer. The model was also applied for the field study of the Biscayne aquifer, Cutler Ridge area near Deering Estate, Florida, USA, to validate the laboratory experiment results.

## 2. Materials and method

### 2.1. Lab-scale case

As presented in Fig. 1, the model setup was 38 cm long, 15 cm deep, and 1 cm wide. The freshwater boundary head was 13.57 cm, while the saline water boundary head was 12.97 cm. This imposed a head difference of dh = 6 mm on the system, which corresponds to a hydraulic gradient of 0.0158.

Abdoulhalik et al., 2017 listed the lab case hydraulic parameters and the boundary conditions as in Table 1. There are two scenarios for the lab-scale problem presented here: a homogeneous scenario, referred to as case H with k = 85 cm/min, and a layered aquifer scenario, referred to hereafter as the HLH case. In this latter scenario, there are three layers with equal thickness, where the hydraulic conductivity of the top and bottom layers was k = 85 cm/min. In contrast, the middle layer had a lower hydraulic conductivity of k = 17 cm/min.

### 2.2. Biscayne aquifer

The finite difference SEAWAT code was applied to the Biscayne aquifer, Cutler Ridge area near Deering Estate, Florida, USA, as a case study to simulate and manage SWI in coastal aquifers influenced by aquifer pumping and saline water abstraction. The aquifer generally is composed of gray, shelly, lightly to moderately cemented limestone with abundant shell fragments or carbonate sand, abundant skeletal moldic porosity, and minor quartz sand. The gray limestone aquifer comprises the Ochopee Limestone of the Tamiami Formation, and, in some areas, the uppermost permeable part of an unnamed formation principally composed of quartz sand. The thickness of the aquifer is comparatively uniform, generally ranging from 30 to 100 feet. The unnamed formation part of the aquifer is up to 20 feet thick (Reese and Cunningham, 2000). The permeability coefficient of 69.44 cm/min. for horizontal and 6.944 cm/min. for vertical hydraulic conductivity were taken. The effective and total porosity of 0.20 and 0.25, respectively, were considered. The longitudinal and transverse dispersivities $\alpha_L$ and $\alpha_T$ were taken as 1000 cm and 100 cm, respectively. The dispersion coefficient in $x$-direction $D_x$ and $y$-direction $D_y$ are considered velocity-dependant. The net recharge is 38 cm (i.e., annual recharge from rainfall), and a constant freshwater flux at this area in the Biscayne aquifer is 5 $m^3$/day (i.e., per meter of shoreline). The densities of freshwater $\rho_f$ and seawater $\rho_s$ were set as 1000 and 1025 kg $m^{-3}$, respectively. Detailed information and other relevant data related to the geologic and hydraulic aspects of the aquifer at Deering Estate were reported by Langevin (2001), as in Table 1.

Fig. 2a illustrates the location map of the Biscayne aquifer that covers an area of 184,500 $m^2$ with an average depth of 33 m below mean sea level. The Figure also shows the hydrostratigraphy of southeastern Florida, the USA, characterised by the shallow surficial and deeper Floridan aquifer systems.

**Table 1**
Hydraulic parameters and boundary conditions of the experimental procedure and Biscayne aquifer.

| Parameters | case study | | Dimension |
|---|---|---|---|
| | lab-scale case | Biscayne aquifer | |
| **Configuration value** | | | |
| X; Z; Y | 0.38; 0.15; 0.01 | 2165; 34; 1 | m |
| **Aquifer Hydraulic Parameters** | | | |
| Freshwater density (ρf) | 1 | 1 | g/L |
| Saltwater density (ρs) | 1.025 | 1.025 | g/L |
| Specific Storage | $10^{-6}$ | $10^{-6}$ | $cm^{-1}$ |
| Porosity | 0.30 | 0.20 | – |
| Longitudinal dispersivity ($\alpha_L$) | 1 | 100 | cm |
| Transverse dispersivity ($\alpha_T$) | 0.05 | 1000 | cm |
| Molecular diffusion coefficient (D*) | 0 | 0 | cm/min |
| Hydraulic conductivity (k) (top and bottom layers) | 85 | 69.44 | cm/min |
| Hydraulic conductivity (k) (middle layer) | 17 | – | cm/min |
| **Aquifer Boundary Condition** | | | |
| Saltwater head ($h_s$) | 0.1297 | 34 | m |
| Initial freshwater head ($h_f$) | 0.1357 | 0.22 | m |
| Sea side concentration ($C_s$) | 36.16 | 35 | g/L |
| Land side concentration ($C_0$) | 0 | 0 | g/L |
| **Cutoff wall configuration** | | | |
| Distance from sea side | 0.66 | 270 | m |
| Opening depth | 0.016 | 4 | m |
| Wall thickness | 0.02 | 0.30 | m |
| Hydraulic conductivity (k) | $1 \times 10^{-5}$ | $1 \times 10^{-5}$ | cm/min |
| **Dam configuration** | | | |
| Distance from sea side | 0.02 | 81 | m |
| Dam height | 0.07 | 17 | m |
| Dam thickness | 0.024 | 0.30 | m |
| Hydraulic conductivity (k) | 0.000017 | 0.000017 | cm/min |
| **Pumping well configuration** | | | |
| Well distance, ($L_w$) | 0.19 | 775 | m |
| Well depth, (Z) | 0.085 | 21 | m |
| Pumping well rates ($Q_{pumping}$) | 0.09; 0.19; 0.29; 0 | 115.74; 173.60; 231.48; 0 | mL/s |

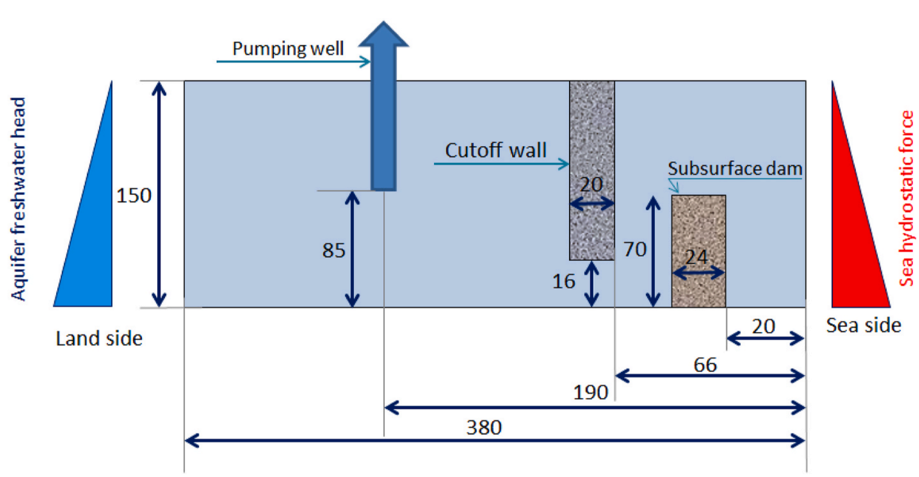


**Fig. 1.** Schematic design of the MPB configuration. The dimensions are in mm.

A fundamental problem in the simulation of karst ground-water flow and solute transport is how best to represent aquifer heterogeneity as defined by the spatial distribution of porosity, permeability, and storage (Cunningham et al., 2006). This highly permeable aquifer principally consists of porous limestone dating from the Pliocene to the Pleistocene. Fig. 2a shows the map of the aquifer cross-section location at the Cutler Ridge area (Langevin, 2001).

A rectangular domain was considered to represent the Biscayne aquifer. The domain had an average length of 2165 km, a thickness of 34 m below the mean sea level (MSL), and a width of 1 m (see Fig. 3). Eighty columns, 1 row, digitised the simulated model domain for the Biscayne aquifer using SEAWAT 4 code, and 34 layers corresponding to a cell dimension of 1 m × 1m x 1m in (ΔxxΔzxΔy), respectively. A constant head of 0.22 mm and concentrations of 35 kg $m^{-3}$ were set along the seaside. A fixed flux boundary condition and a null concentration were set on the land side.

### 2.3. SEAWAT model

A combined MODFLOW-2000 (Harbaugh et al., 2000) and MT3DMS (Zheng and Wang, 1999) simulations were developed to build a 3D SEAWAT model. The third version of SEAWAT-2000 is documented by (Langevin et al., 2003). The current study used SEAWAT V4, which was designed to compute fluid density and viscosity (Langevin et al., 2008). The model is to examine the performance of freshwater abstraction on SWI in the coastal aquifer for the experimental scale aquifer and the field scale Biscayne aquifer.

SEAWAT V4 has two new processes, including the Variable-Density Flow (VDF) process for solving the variable-density groundwater flow equation according to the equivalent freshwater head written by Guo and Langevin (2002). Eq. (1):

*I am running a few minutes late; my previous meeting is running over.*

$$\text{I am running a few minutes late; my previous meeting is running over.}\nabla\left[\rho^*\frac{\mu_o}{\mu}{}^*K_o\left(\nabla^*h_0+\frac{\rho-\rho_f}{\rho_f}{}^*\nabla Z\right)\right]=\rho^*S_{S,0}\left(\frac{\partial h_O}{\partial t}\right)+\theta^*\left(\frac{\partial\rho}{\partial C}\right)\left(\frac{\partial C}{\partial t}\right)-\rho_s{}^*q_s \tag{1}$$

The other process is the Integrated MT3DMS Transport (IMT), which solving the advection-dispersion equation (Zheng and Wang, 1999), Eq. (2):

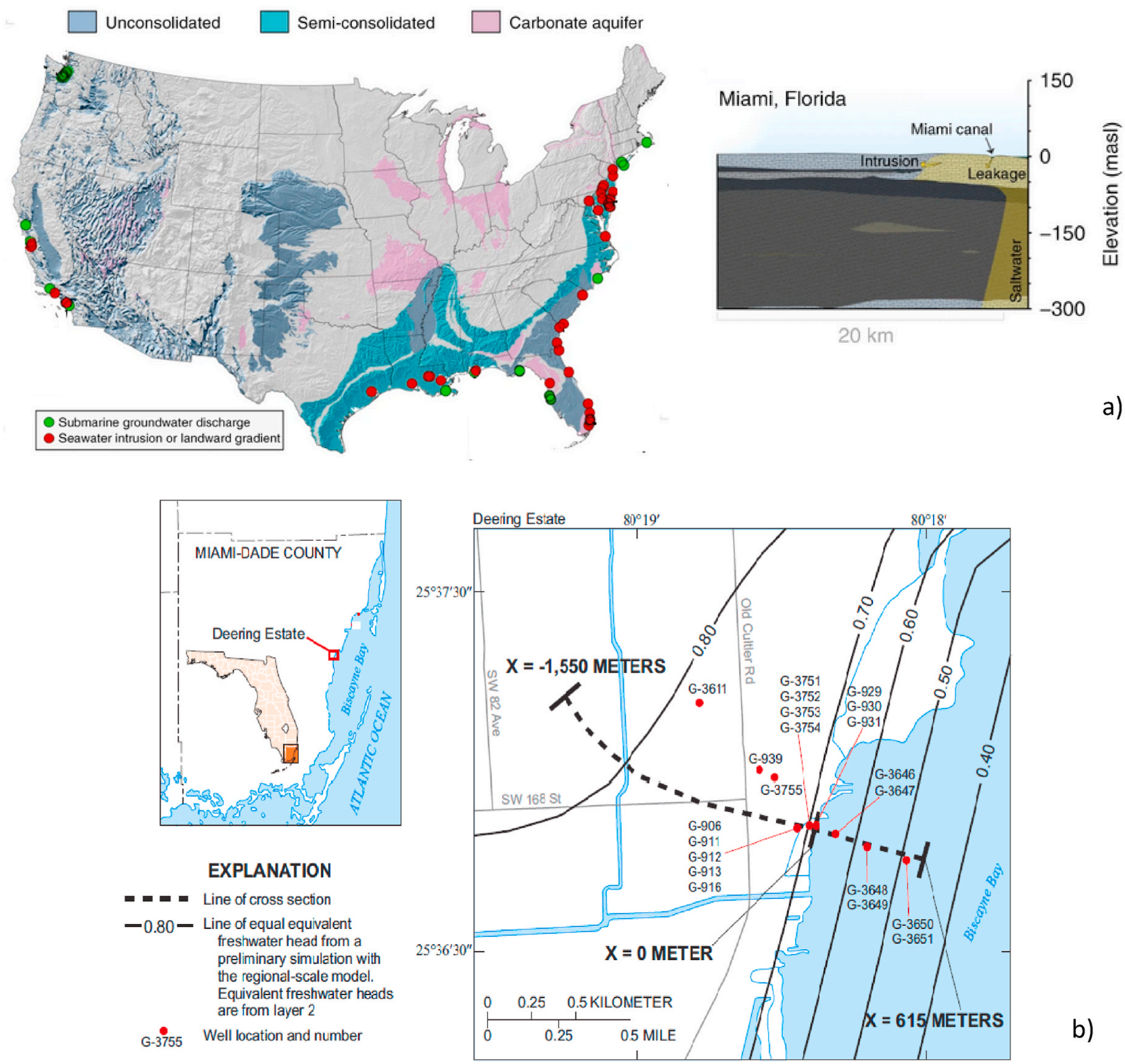


**Fig. 2.** Biscayne Aquifer, Florida, USA a) near Miami (Renken et al., 2005; Prinos et al., 2016) (Florida), a shallow carbonate aquifer (Biscayne) has experienced seawater intrusion, likely exacerbated by the construction of leaky canals (Jasechko et al., 2020) and b) study site location adapted after Langevin (2003).

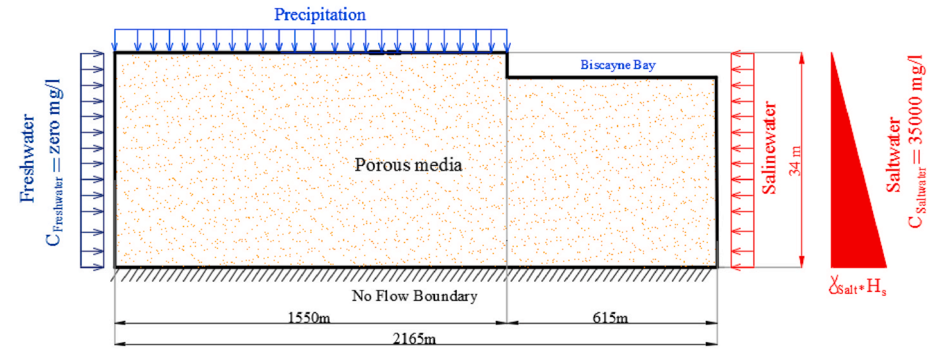


**Fig. 3.** Definition sketch and boundary conditions for Biscayne aquifer

$$\left(1+\frac{\rho_b K_d^k}{\theta}\right)\left(\frac{\partial(\theta C^k)}{\partial t}\right)=\nabla\left[\theta\left(D_m{}^k+\alpha\frac{q}{\theta}\right).\nabla C^k\right]-\nabla.(qC^k)-q_s^{*}C_s^k \qquad (2)$$

Where $\rho_0$: fluid density [$ML^{-3}$]; μ: dynamic viscosity [$ML^{-1}T^{-1}$]; $h_0$: hydraulic head [L]; $K_0$: the hydraulic conductivity [$LT^{-1}$]; $S_{s,0}$: specific storage [$L^{-1}$]; t: is time [T]; θ: porosity [−]; C: salt concentration [$ML^{-3}$]; $q'_s$: is a source or sink [$T^{-1}$]; of fluid with density $\rho_s$; $\rho_b$: is the bulk density [$ML^{-3}$]; $K_d^k$: distribution coefficient of species k [$L^3M^{-1}$]; $C^k$: concentration of species k [$ML^{-3}$]; D: hydrodynamic dispersion coefficient tensor [$L^2T^{-1}$]; q: specific discharge [$LT^{-1}$]; and $C_s^k$: source or sink concentration [$ML^{-3}$] of species k.

## 3. Results and discussion

Both models for the test case and the real case of the Biscayne aquifer, Cutler Ridge area near Deering Estate, Florida, USA, were simulated in the current study.

### 3.1. Impact of mixed physical barriers on SWI (no pumping well)

The experimental test case has the cutoff wall at 6.60 cm from the seaside, the wall opening (the distance from the bottom of the aquifer to the tip of the wall where water can flow through) was 1.60 cm, the wall thickness was 2 cm, the hydraulic conductivity was $1.0\times10^{-5}$ cm/min. The subsurface dam was installed at 2 cm from the seaside with a thickness of 2.40 cm, the dam height was 7 cm from the base of the aquifer, and the hydraulic conductivity was $1.7\times10^{-5}$ cm/min.

The Numerical seawater wedge length reached 7.1 cm from the seaside for the homogenous case (Fig. 4a) compared to the 7.0 cm obtained from the experimental results published by Abdoulhalik et al. (2024) as in Fig. 4b. This is for the case of no pumping wells. Fig. 4 c and d show a different scenario of a three-layered aquifer of equal depth, with the hydraulic conductivity of the middle interlayer reduced to 17.00 cm/min and that of the bottom and top layers equalled 85 cm/min. The numerical SWI wedge for this layered scenario reached 6.90 cm compared to experimental results of 6.80 cm, as published by Abdoulhalik et al. (2024). Again, there is no pumping well in this case too.

### 3.2. Impact of pumping well on the MPB performance for the lab-scale case

Fig. 5 shows the results of the homogeneous and layered scenarios, where the MPB performance was examined at different pumping rates

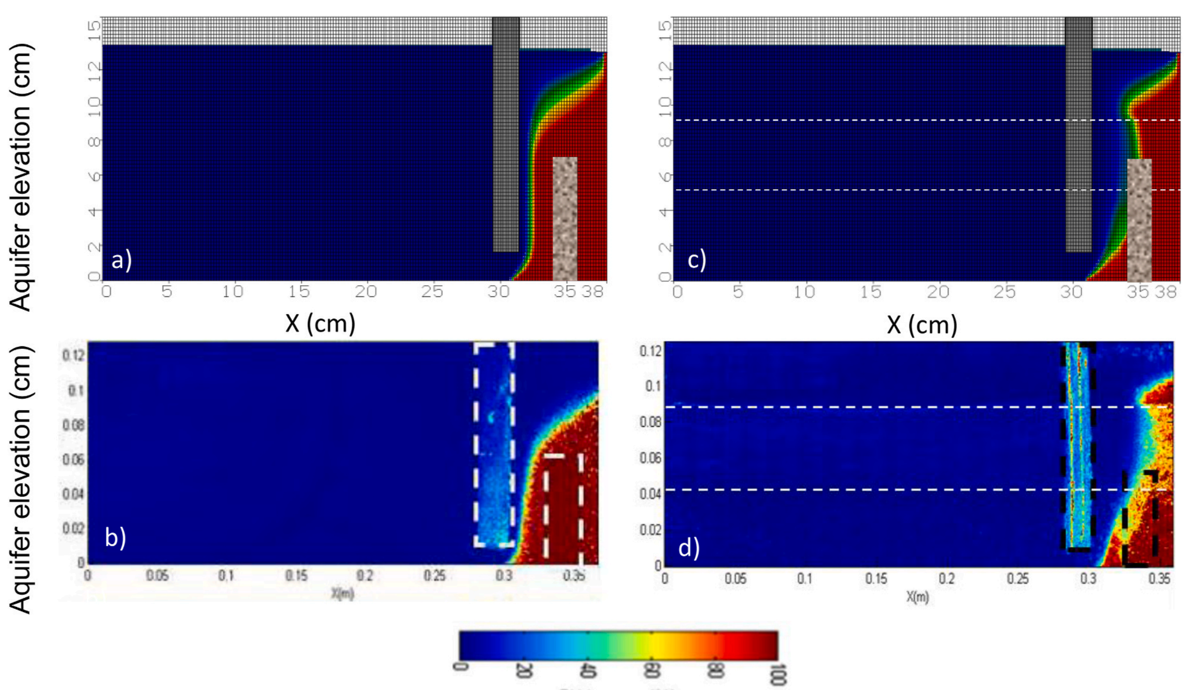


**Fig. 4.** Salinity results are obtained by (a) SEAWAT (top) for homogenous cases and (b) experimental for homogenous case (Abdoulhalik et al., 2024). (c) SEAWAT for the heterogeneous case and (d) experimental heterogeneous case (Abdoulhalik et al., 2024). There is no pumping in this scenario

that gradually increased. The times in Fig. 5 are for the shape of the SWI wedge at the quasi-steady state, where the upconing started and the seawater reached the bore of the well. This was the time when the well started to be contaminated with seawater. These shown times are in minutes and counted from the change of abstraction rates for each case; for the bottom case in the figure, the time is counted after the pump was switched off. The pumping well rates were examined at $Q_1 = 0.09$ ml/s, $Q_2 = 0.19$ ml/s, and $Q_3 = 0.29$ ml/s, as shown in the figure. The well was installed 19 cm from the seaside, and the depth from the aquifer bed was 8.50 cm. After that, the pumping was switched off to show the SWI during the retreat. For the homogeneous aquifer (Fig. 5, left column), the SWI wedge intrusion under pumping conditions reached 10.40 cm, 18.50 cm and 21.80 cm for $Q_1$, $Q_2$, and $Q_3$, respectively, compared with 7.10 cm in the base case without pumping that was presented in Fig. 4. Thus, for the homogeneous aquifer, the percentage of SWI increased by 46%, 161% and 207%, for $Q_1$, $Q_2$, and $Q_3$, respectively, compared to the case with no pumping. Also the aquifer salt variation **(L - L$_o$)/L$_o$** were calculated to check the aquifer salt situation, which the positive sign indicates that the aquifer salt is greater than the base case and this has a negative impact to salt removal, while the negative sign indicates that the aquifer boundary conditions or physical subsurface barriers have a positive effect on saltwater intrusion. $L_o$ is the initial saltwater intrusion length at the base case and L is the initial saltwater intrusion length at the proposed case.

The layered aquifer results (Fig. 5, right column) showed that the intrusion reached 8.80 cm, 15.30 cm and 21.10 cm, respectively, compared to 6.90 cm in the base case without pumping. This represents a percentage increase of the SWI by 28%, 122% and 206%, respectively

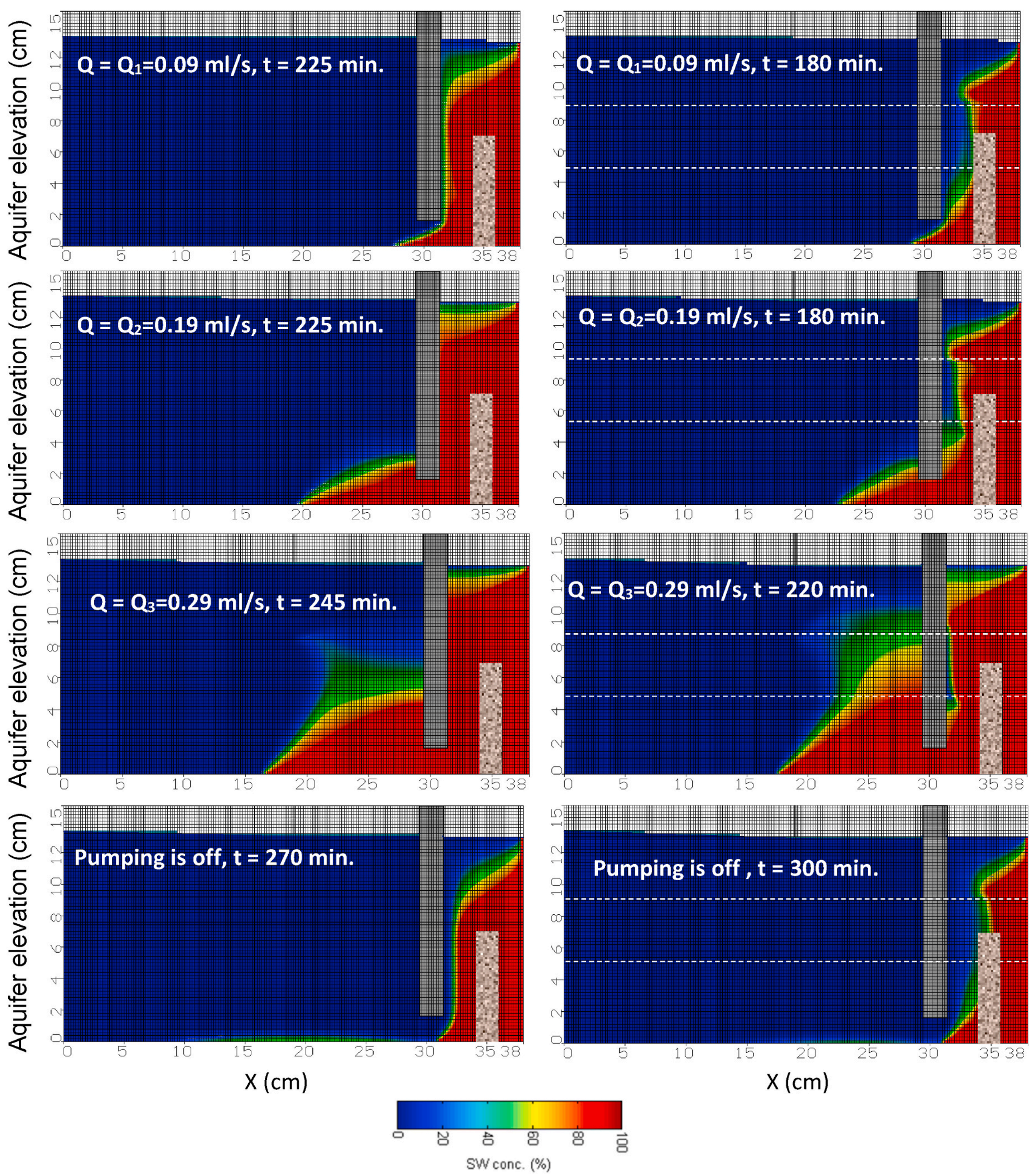


Fig. 5. Lab-scale case results of concentration colour map of the transient saltwater wedge during the pumping conditions and after pumping is switched off for homogenous cases (left) and heterogeneous (right). The time when seawater upconing starts is the time shown for each case.

(Fig. 9a). Results showed that the SWI wedge extended further inland in the homogenous aquifers greater than in the heterogeneous aquifer. The highest aquifer salinity was obtained for the third scenario (Q = 0.29 ml/s).

After the pumping well was switched off, the SWI for the homogenous and layered aquifers reached 7.20 cm and 7 cm, respectively. This represents a percentage increase of SWI by 1.41% and 1.45%, respectively, compared to the base case (Fig. 9a).

### 3.3. Impact of additional layered scenarios

In this section, we compared three different layered configurations with the homogeneous case. In these cases, we used Q3 = 0.29 ml/s, which was the highest rate we used in the previous scenarios. In addition to the homogeneous scenario in Fig. 6, we examined the layered cases where the low-k layer existed at the top of the aquifer (case LH), in the middle of the aquifer (case HLH), and at the bottom of the aquifer (case HL). Like the above scenarios, the low-K was set at 17 cm/min while the aquifer hydraulic conductivity was 85 cm/min. So, the low-K was one-fifth of the aquifer conductivity.

The SWI wedge length was 19.5 cm, 21.1 cm, and 18.80 cm for case LH, case HLH, and case HL, respectively, compared to 21.80 cm in the homogeneous scenario. The existence of a low permeability layer at the bottom of the aquifer reduced the intrusion length, and it also took a much longer time, in this case, for the seawater to reach the bore of the well.

The results agreed with those of Antoifi and Ahmed, (2017). The results also showed that the presence of an interlayer of low k (case HLH) inhibited the downward movement of the freshwater towards the wall opening, thus decreasing the repulsion ability of the wall. Moreover, the presence of an underlying low permeability layer (case HL) was found to obstruct the freshwater flow in the lower part of the aquifer, thereby slowing down the velocity through the wall opening.

### 3.4. Application of MPB on SWI for field homogenous aquifer

Moreover, this study simulated the field case for the homogenous Biscayne aquifer. The results of the current simulated model (Fig. 7a) were compared with Langevin (2003). The model was calibrated by adjusting aquifer parameters and the boundary stresses within a range of reasonable values, and the calculated values generally matched those with field data obtained from 21 monitoring wells to monitor the concentration of total dissolved solids obtained from Langevin (2001). The calibration procedure is estimated and illustrated in Fig. 7a.

The calibration process yielded insightful results. A root mean square and a normalised root mean square of 2062.31 ppm and 6.61%, respectively, between the observed and calculated salinity. This metric is particularly valuable as it gauges the relative accuracy of the model in the context of the observed data variability (Chai and Draxler, 2014). The residuals, representing the differences between observed and simulated values, ranged from −5552 ppm to 388.30 ppm. The mean residual was calculated at 398.93 ppm, providing an absolute residual mean of 1727.13 ppm. Additionally, the standard error of the estimate was quantified at 441.53 ppm. The SWI reached 428 m from the shoreline at X = −428 for the case without an MPB barrier as shown in Fig. 7b. The aquifer salt mass reached 121582 ppm using MPB compare with 167357 ppm at the baseline case. The aquifer salt variation were calculated using **$(C\text{-}C_0)/C_0$**, where $C_0$ is the initial salt concentration and C is the salt concentration,the positive sign indicated that the aquifer salt is more than the base case while the negative sign represents a positive effect on saltwater intrusion (Abd-Elaty et al., 2019).

For the MPB in this field case of Biscayne aquifer, the cutoff wall hydraulic conductivity was $1 \times 10^{-5}$ cm/min; the wall opening depth was 4m (distance from the toe of the wall and aquifer bottom line), while the wall thickness was set at 0.30 m, and the wall distance was 270 m from the shoreline, so at X = −270 (shoreline is at X = 0). The subsurface dam was set at 81 m from the shoreline at X = −81 with a width of 0.30 m and a height of 17 m from the aquifer base. The dam's hydraulic conductivity was 0.000017 cm/min. The SWI reached 35 m from the shoreline at X = +35 after the installation of the MPB as shown in Fig. 7c

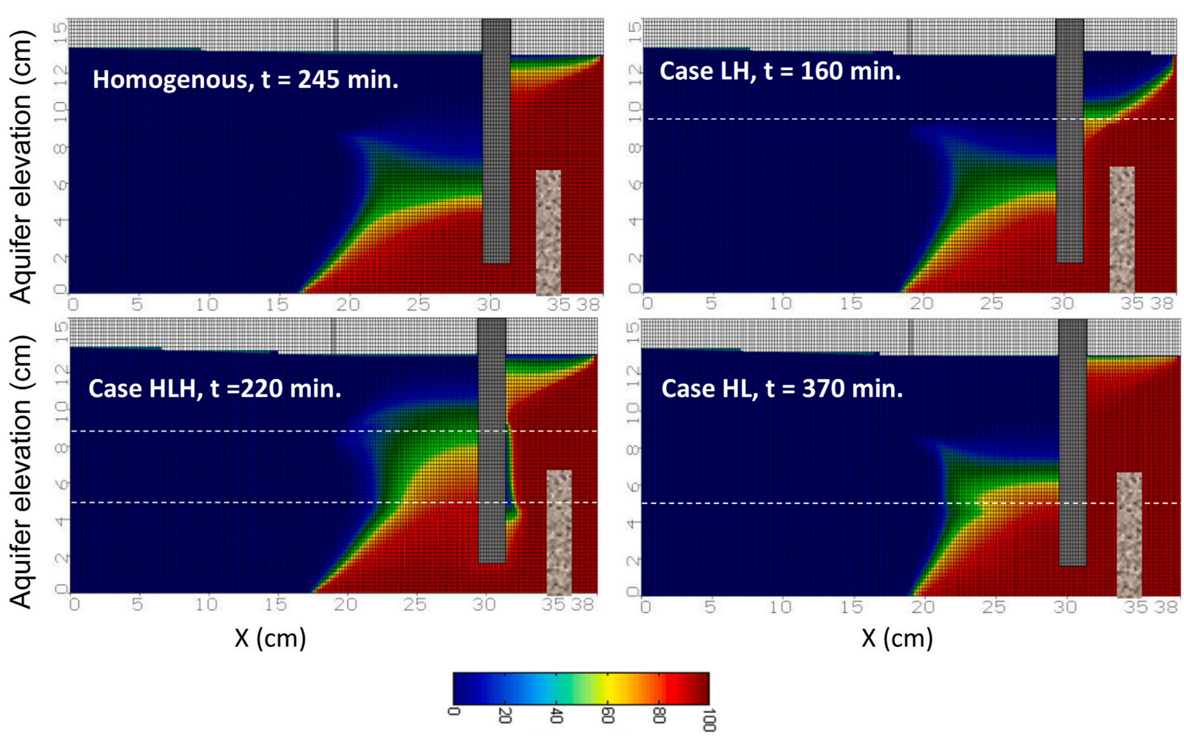


**Fig. 6.** Lab-scale case concentration colour map of the transient saltwater wedge under pumping conditions Q = Q3 = 0.29 ml/s for layered aquifer

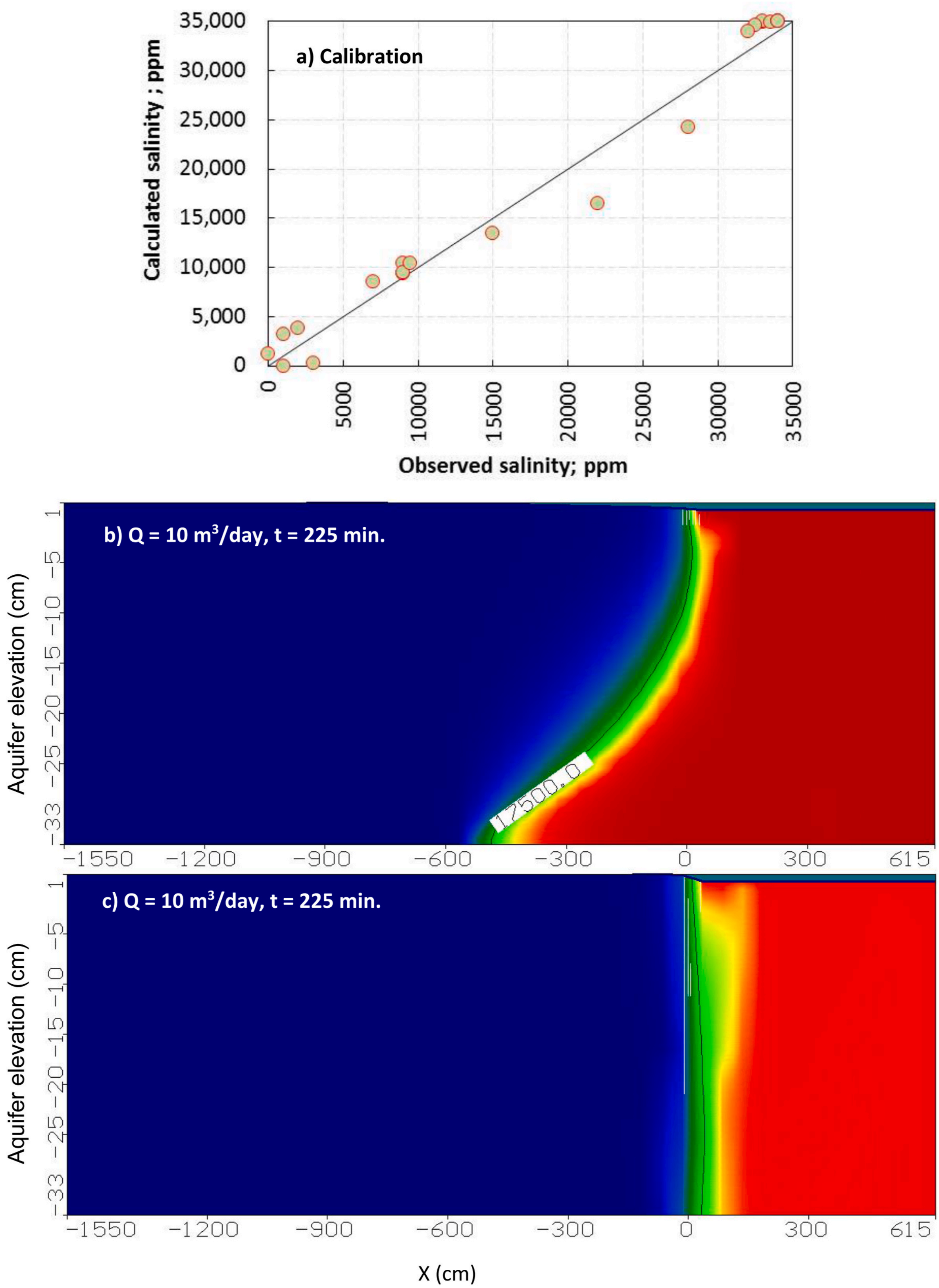


**Fig. 7.** Salinity results of Biscayne aquifer for A) calibration between the field data and SEAWAT, (b) the homogenous case for the baseline case (case of no barrier) and (c) MPB case

compared with 428 m from the shoreline at X = −428 for the case without an MPB barrier. Various methods are employed to mitigate SWI, including hydraulic and physical barrier approaches. In the Biscayne aquifer, a 3D SEAWAT model was used to assess the SWI exacerbated by the impact of increasing the abstraction pumping due to future population growth.

For the pumping rates conditions in the real case aquifer, the pumping wells were installed at 775 m from the shoreline at X = −775 and a depth of 21m from the aquifer base with pumping rates of 10 $m^3$/day, 15 $m^3$/day and 20 $m^3$/day. The modelling results indicated that the aquifer salinity after the installation of a pumping well reached 21m (X=-21), 484 m (X=-484) and 1110 m (X=-1110), respectively (Fig. 8), compared with 35 m (X=+35) at the baseline case without pumping conditions by using MPB barrier and measured from the shoreline (X = 0).

For a real case of the Biscayne aquifer, the groundwater salinity was incresed and reached +3%, +38%, and +121% by increasing the abstraction well rates to 10 $m^3$/day, 15 $m^3$/day, and 20 $m^3$/day compared with no pumping at the baseline case and MPB barrier (Fig. 9b). For the turnoff case, the pumping rates were 0 $m^3$/day, and the intrusion was 32 m from the shoreline at X = +32; the changing in SWI reached +1.60%.

## 4. Discussion

Previous studies investigated using single physical subsurface barriers such as cutoff walls, subsurface dams, and combinations of the two using mixed physical barriers (MPB). Research about the impact of applying MPB in homogenous and layered aquifers without pumping conditions was developed, and more studies were published, while the

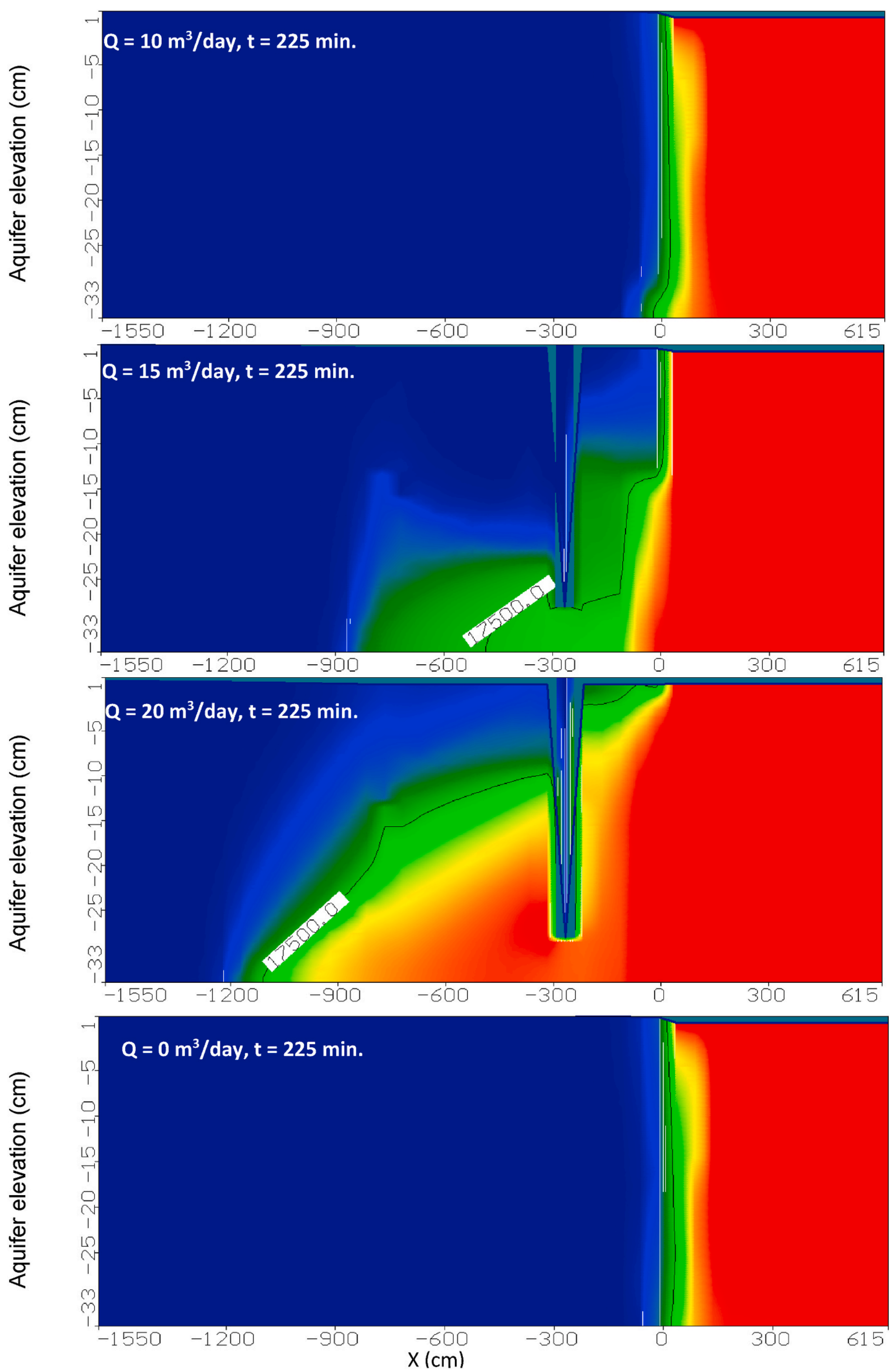


**Fig. 8.** Numerical results concentration colour map of the saltwater wedge before the pump and under pumping conditions for homogenous cases

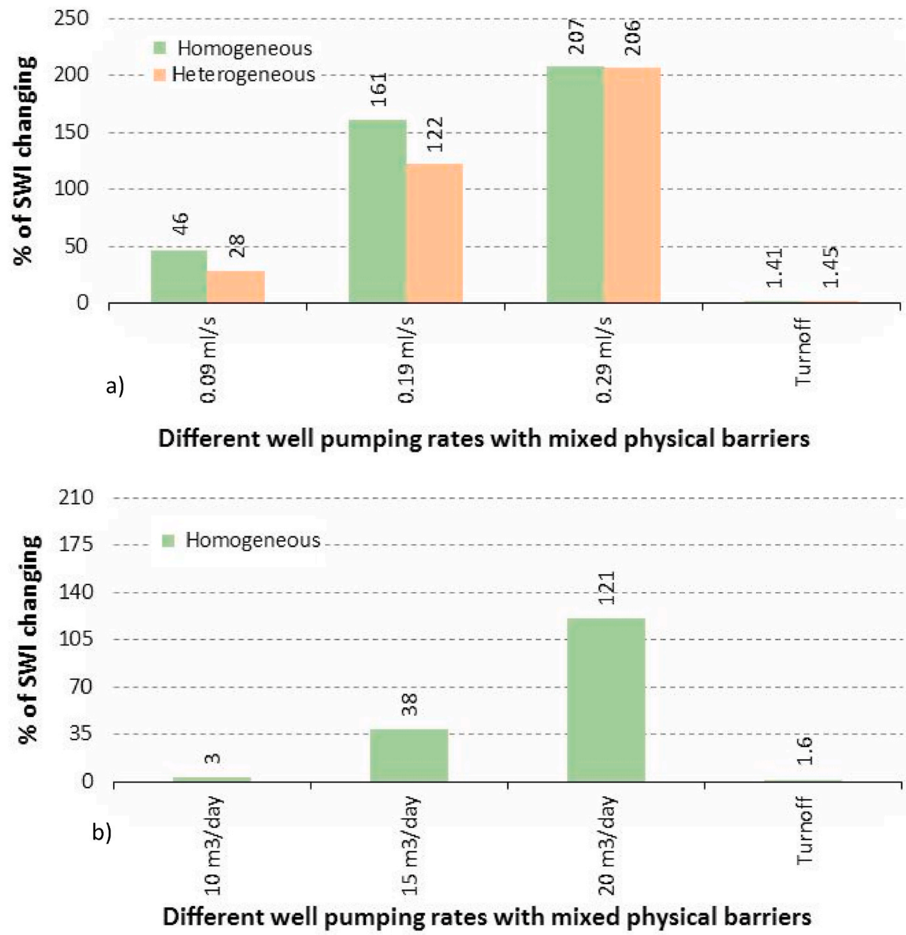


**Fig. 9.** The % of aquifer salinity for well pumping rates cases in a) the homogenous and heterogeneous cases of experimental and (b) a real case of homogenous Biscayne aquifer.

application of MPB in homogenous and layered aquifers under pumping conditions is limited.

The current study investigated the impact of using MPB in homogenous and layered aquifers on SWI under pumping conditions. The study used the test case for homogenous and layered aquifers, while a real case of homogenous Biscayne aquifer, Florida, USA, was applied to investigate the effect of MPB to control SWI.

The test case results for homogenous and layered aquifers showed that the SWI increased with the well pumping rates. Also, the SWI results in layered aquifers produced wedge lengths smaller than the homogenous coastal aquifers.

The installation of an MPB under the pumping conditions for a homogenous aquifer in the field case of the Biscayne Aquifer, Florida, USA agrees with the results published by Abdoulhalik et al., 2017 who developed a mixed physical barrier (MPB) as a new SWI control method, combining a cutoff wall and a semi-permeable subsurface dam without pumping conditions. SWI length was reduced by 62% and 42% for using the MPB compared with the semi-permeable dam and the single cutoff wall. Gao et al. (2021) showed that the efficiency of using MPB in removing residual saltwater could be 40% to 100% and 0% to 56% higher than that of traditional subsurface dams and cutoff walls, respectively. Wang et al. (2023) used MPB to mitigate the SWI in coastal unconfined aquifers and found it 46–53% and 16–57% more effectively than traditional subsurface dams and cutoff walls, respectively. However, the construction of the MPB resulted in more severe nitrate pollution accumulation. Specifically, the MPB induced 14–27% and 2–12% more nitrate accumulation than conventional subsurface dams and cutoff walls. Abdoulhalik et al. (2024) used the MPB in layered aquifer for SWI management. The results showed that the SWI was mitigated by 71% and 69% for experimental and numerical results, respectively, compared with the single cutoff wall. Emara et al. (2024) applied a numerical study for investigate the efficiency of MPB for SWI removal in coastal heterogeneous aquifers. The results showed that MPBs efficiently decreased the SWI penetration length in the investigated cases. The reductions in penetration length were up to 65% in all cases.

The current study's shows the requirement to apply the feasibility study for using the MPB in more homogenous and layered real field heterogeneous aquifers. Application of this method in a 3D model is required to confirm the numerical and experimental results in the same coastal aquifer conditions worldwide.

## 5. Summary and conclusions

The current study used the mixed physical barriers (MPB) to study saltwater intrusion in coastal aquifers. The SEAWAT code investigated aquifer salinity in homogeneous and layered heterogeneous aquifers under pumping conditions.

1. The SWI for the two-dimensional (2D) laboratory tests under pumping conditions reached 10.40 cm, 18.50 cm and 21.80 cm compared with 7.10 cm in the baseline case without pumping using pumping rates of 0.09 mg/l, 0.19 mg/l and 0.29 mg/l, respectively, for the homogenous aquifer. The SWI for the layered heterogeneous aquifer results reached 8.80 cm, 15.30 cm and 21.10 cm under the

same pumping rates, respectively, compared to 6.90 cm in the baseline case without pumping.

2. For an aquifer with top low-k layer, the SWI was reduced to 19.50 cm compared with 21.80 cm in the homogenous case. In the aquifer with the middle low-k layer, the SWI reached 21.10 cm, while it reached 18.80 cm for the aquifer with the bottom low k layer. These cases were for the laboratory tests.
3. For the real field case, the SWI reached -35 m from the shoreline at X=+35 after the installation of the MPB barrier compared with 428 m (X=-428) for the case without an MPB barrier. Morover, the salinity was incresed and reached 21 m (X=-21), 484 m (X=-484) and 1110 m (X=-1110), with pumping rates of 10 $m^3$/day, 15 $m^3$/day and 20 $m^3$/day, respectively, compared with 35 m (X=+35) under pumping conditions and measured from the shoreline (X = 0).

The study results are novel for applying the MPB in homogeneous and layered heterogeneous aquifers under pumping conditions. The limitations of this study are that it requires more field applications to move beyond the experimental laboratory model. Also, economic feasibility is essential to compare the use of single physical barriers and MPB.

## CRediT authorship contribution statement

**Ismail Abd-Elaty:** Writing – review & editing, Writing – original draft, Visualization, Validation, Supervision, Software, Resources, Project administration, Methodology, Investigation, Formal analysis, Data curation, Conceptualization. **Ashraf Ahmed:** Writing – review & editing, Writing – original draft, Visualization, Validation, Supervision, Software, Resources, Project administration, Methodology, Investigation, Funding acquisition, Formal analysis, Data curation, Conceptualization.

## Declaration of competing interest

The authors declare that they have no known competing financial interests or personal relationships that could have appeared to influence the work reported in this paper.

## Data availability

No data was used for the research described in the article.

## References


Abd-Elaty, I., Sallam, G., Strafacec, S., Scozzari, A., 2019. Effects of climate change on the design of subsurface drainage systems in coastal aquifers in arid/semi-arid regions: Case study of the Nile delta. Science of the Total Environment Journal 672, 283–295. https://doi.org/10.1016/j.scitotenv.2019.03.483.

Abd-Elaty, I., Shahawy, A.E., Santoro, S., Curcio, E., Straface, S., 2021. Effects of groundwater abstraction and desalination brine deep injection on a coastal aquifer. Sci. Total Environ. 795, 148928.

Abd-Elaty, I., Pugliese, L., Straface, S., 2022. Inclined physical subsurface barriers for saltwater intrusion management in coastal aquifers. Water Resour. Manag. 36, 2973–2987. https://doi.org/10.1007/s11269-022-03156-7.

Abd-Elaty, I., Kuriqi, A., Ahmed, A., 2024. Effectiveness of different mixed physical barriers in controlling seawater intrusion in homogeneous and layered coastal aquifers. Groundwater for Sustainable Development 27, 101318.

Abdoulhalik, A., Abdelgawad, A.M., Ahmed, A., Moutari, S., Hamill, G., 2022. Assessing the protective effect of cutoff walls on groundwater pumping against saltwater upconing in coastal aquifers. J. Environ. Manag. 323, 116200. https://doi.org/10.1016/j.jenvman.2022.116200.

Abdoulhalik, A., Ahmed, A., Abd-Elaty, I., 2024. Effects of layered heterogeneity on mixed physical barrier performance to prevent seawater intrusion in coastal aquifers. J. Hydrol. 637, 131343. https://doi.org/10.1016/j.jhydrol.2024.131343. ISSN 0022-1694.

Abdoulhalik, A., Ahmed, A., Hamill, G.A., 2017. A new physical barrier system for seawater intrusion control. J. Hydrol. 549, 416–427.

Agren, J., Svensson, R., 2007. Postglacial land uplift model and system definition for the new Swedish height system RG 2000. In: LMV-rapport 2007:4, Rapportserie: Geodesi och Geografiska informationssystem. Lantmäteriet, Gävle, Sweden.

Antoifi, Abdoulhalik, Ahmed, Ashraf A., 2017. The effectiveness of cutoff walls to control saltwater intrusion in multi-layered coastal aquifers: experimental and numerical study. J. Environ. Manag. 199, 62–73. https://doi.org/10.1016/j.jenvman.2017.05.040. ISSN 0301-4797.

Badan Ghyben, W., 1889. Nota in verband met de voorgenomen putboring nabij Amsterdam. Tijdshrift van het koninklyk Instituut van Ingenieurs 21.

Chai, T., Draxler, RRJGmdd, 2014. Root Mean Square Error (RMSE) or Mean Absolute Error (MAE), vol. 7, pp. 1525–1534.

Cheng, J.-R., Strobl, R.O., Yeh, G.-T., Lin, H.-C., Choi, W.H., 1998. Modeling of 2D density-dependent flow and transport in the subsurface. J. Hydrol. Eng. 3 (4), 248–257.

Cunningham, K.J., Wacker, M.A., Robinson, E., Dixon, J.F., Wingard, G.L., 2006. A Cyclostratigraphic and Bore¬hole-Geophysical Approach to Development of a Three-Dimen-Sional Conceptual Hydrogeologic Model of the Karstic Biscayne Aquifer, Southeastern Florida. Geological Survey Scien¬tific Investigations USA.

Emara, S.R., Armanuos, A.M., Zeidan, B.A., Gado, T.A., 2024. Numerical investigation of mixed physical barriers for saltwater removal in coastal heterogeneous aquifers. Environ. Sci. Pollut. Control Ser. 31, 4826–4847. https://doi.org/10.1007/s11356-023-31454-z.

Fahs, M., Koohbor, B., Belfort, B., Ataie-Ashtiani, B., Simmons, C.T., Younes, A., Ackerer, P., 2018. A Generalized Semi-analytical Solution for the Dispersive Henry Problem: Effect of Stratication and Anisotropy on Seawater Intrusion.

El Fleet, M., Baird, J., 2001. The development and application of groundwater models to simulate the behaviour of groundwater resources in the Tripoli aquifer, Libya. Proceeding of the 1st International Conference and Workshop on Saltwater Intrusion and Coastal Aquifers, Monitoring, Modelling, and Management. Citeseer.

Frind, E.O., 1982. Simulation of long-term transient density-dependent transport in groundwater. Adv. Water Resour. 5 (2), 73–88. https://doi.org/10.1016/0309-1708(82)90049-5.

Gao, M., Zheng, T., Chang, Q., Zheng, X., Walther, M., 2021. Effects of mixed physical barrier on residual saltwater removal and groundwater discharge in coastal aquifers. Hydrol. Process. 35 (7). https://doi.org/10.1002/hyp.14263. Article e14263.

Gao, S., Zheng, T., Zheng, X., Walther, M., 2022. Influence of layered heterogeneity on nitrate accumulation induced700 by cutoff wall in coastal aquifers. J. Hydrol. 609, 127722. https://doi.org/10.1016/j.jhydrol.2022.127722.

Goswami, G., Rai, A.K., 2024. Identifying intrusion of seawater in coastal aquifers by modified GALDIT (M-GALDIT) index. Groundwater for Sustainable Development 25 (2024), 101173. https://doi.org/10.1016/j.gsd.2024.101173. ISSN 2352-801X.

Guo, W., Langevin, C.D., 2002. User's Guide to SEAWAT; a Computer Program for Simulation of Three-Dimensional Variable-Density Groundwater Flow.

Harbaugh, A.W., Banta, E.R., Hill, M.C., McDonald, M.G., 2000. MODFLOW-2000, the U. S. Geological Survey Modular Groundwater Model – User Guide to Modularization Concepts and the Groundwater Flow Process, vols. 2000–92. U.S. Geological Survey Open-File Report, Reston, Virginia. http://pubs.er.usgs.gov/usgspubs/ofr/ofr200092. September 2010.

Henry, H.R., 1964. Effects of dispersion on salt encroachment in coastal aquifers. " Seawater in Coastal Aquifers". US Geological Survey, Water Supply Paper 1613, C70–C80.

Jasechko, S., Perrone, D., Seybold, H., et al., 2020. Groundwater level observations in 250,000 coastal US wells reveal scope of potential seawater intrusion. Nat. Commun. 11, 3229. https://doi.org/10.1038/s41467-020-17038-2.

Langevin, C.D., 2003. Simulation of submarine ground water discharge to a marine estuary: Biscayne Bay, Florida. Groundwater 41 (6), 758–771. https://doi.org/10.1111/j.1745-6584.2003.tb02417.x.

Langevin, C.D., Thorne, Jr D.T., Dausman, A.M., Sukop, M.C., Guo, W., 2008. SEAWAT Version 4: a Computer Program for Simulation of Multi-Species Solute and Heat Transport, vols. 2328–7055. Geological Survey (US).

Manga, M., et al., 2012. Changes in permeability caused by transient stresses: field observations, experiments, and mechanisms. Rev. Geophys. 50 (2). https://doi.org/10.1029/2011RG000382.

Mays, D.C., 2010. Contrasting clogging in granular media filters, soils, and dead-end membranes. Journal of environmental engineering 136 (5), 475–480.

Mueller, W., Zamrsky, D., Essink, G.O., et al., 2024. Saltwater intrusion and human health risks for coastal populations under 2050 climate scenarios. Sci. Rep. 14, 15881. https://doi.org/10.1038/s41598-024-66956-4.

Ojeda, C., Gallardo, P., Hita, L., Arteaga, L., 2004. Saline interface of the yucatan peninsula aquifer. Proceedings of the 18th Salt Water Intrusion Meeting.

Panthi, J., Pradhanang, S.M., Nolte, A., Boving, T.B., 2022. Saltwater intrusion into coastal aquifers in the contiguous United States - a systematic review of investigation approaches and monitoring networks. Sci. Total Environ. 836 (2022), 155641. https://doi.org/10.1016/j.scitotenv.2022.155641. ISSN 0048-9697.

Pisinaras, V., Paraskevas, C., Panagopoulos, A., 2021. Investigating the effects of agricultural water management in a mediterranean coastal aquifer under current and projected climate conditions. Water 13 (1), 108.

Pool, M., Carrera, J., 2010. Dynamics of negative hydraulic barriers to prevent seawater intrusion. Hydrogeol. J. 18, 95–105. https://doi.org/10.1007/s10040-009-0516-1.

Reese, R.S., Cunningham, K.J., 2000. Hydrogeology of the Gray Limestone Aquifer in Southern Florida. Geological Survey Water-Resources Investigations, USA.

Taylor, A., Hulme, P., Hughes, A., Foot, S., 2001. Benchmarking of variable density model codes against Henry's problem. Water 10 (2), 230. https://doi.org/10.3390/w10020230.

Wang, J., Kong, J., Gao, Zhou L., 2023. Effect of mixed physical barrier on seawater intrusion and nitrate accumulation in coastal unconfined aquifers. Environ. Sci. Pollut. Res. 30, 105308–105328. https://doi.org/10.1007/s11356-023-29637-9.

Zheng, C., Wang, P.P., 1999. MT3DMS: a modular three-dimensional multispecies transport model for simulation of advection, dispersion. And Chemical Reactions of Contaminants in Groundwater Systems; Documentation and User's Guide.

Zheng, H., et al., 2021. Optimal location of cutoff walls for seawater intrusion. Appl. Water Sci. 11 (11), 179. https://doi.org/10.1007/s13201-021-01514-1.